A new simplified meta-model to evaluate the transmission of ground movements to structures integrating the elastoplastic soil behavior

Elio El Kahi, Olivier Deck, Michel Khouri, Rasool Mehdizadeh, Pierre Rahmé

A new simplified meta-model to evaluate the transmission of ground movements to structures integrating the elastoplastic soil behavior

Elio EL KAHI[12*], Olivier DECK[1], Michel KHOURI[2], Rasool MEHDIZADEH[1], Pierre RAHME[2]

[1] *Lorraine University, CNRS, CREGU, GeoRessources laboratory, Ecole des Mines de Nancy, Campus Artem, CS14234, 54042 Nancy Cedex, France*
[2] *Faculty of Engineering, Lebanese University, Roumieh, Mount-Lebanon, Lebanon*

Abstract

Many buildings may suffer damage due to ground movements associated to underground excavations like tunneling, mines or urban excavations. The level of damage depends upon the rate of ground movements transmitted to structures that is affected by the Soil-Structure Interaction (SSI) conditions and parameters such as the soil elastoplastic behavior. The purpose of this paper is to integrate the soil elastoplasticity while investigating the response of a structure sitting on a soil subjected to a ground movement. Analytical and numerical approaches are applied to examine the effect of the non-linear soil behavior. The analytical approach is based on modified Winkler and Pasternak elastic models under the assumption of limiting the soil reaction by its bearing capacity ; the numerical approach is based on finite element models, using Plaxis 2D that consider an elastoplastic soil behavior. Results display the discrepancy in the structural response between considering an elastic or an elastoplastic soil behavior. Based on a significant number of iterations, the artificial neural network technique is used to propose a new simplified meta-model that integrates the soil elastoplasticity to evaluate the transmission of ground movements to structures. In addition, a procedure, which can be used by engineers and designers, is developed to evaluate the transmission ratio for any structure sitting on any type of soil.

Keywords

Meta-model, elastoplastic soil behavior, Pasternak model, Winkler model, soil-structure interaction, ground movements, artificial neural network.

1. Introduction

Ground movements designate a sequence of soil displacements, of natural or anthropogenic origin such as shrink-swell phenomenon of clayey soils, influence of nearby excavations (tunnels) and presence of underground voids such as mining subsidence and sinkholes. These ground movements are responsible of the soil settlements and displacements. The soil displacement may occur even in the absence of any structure on top of it; this case represents the free-field ground movement. Conversely,

if the soil is underneath an existing structure, the ground movement is transmitted to the building foundations (Figure 1). An important parameter is the stiffness and the building stiffness could be underestimated if it is only based on the foundation geometry. Consequently, the building with its foundation is assimilated to a beam with an equivalent stiffness. The computed deflection represents the deflection transmitted to both the building and its foundation which may cause a structural damage [1, 2]. It is not proper to consider that these movements in the free-field are transmitted entirely to the building since the transmission may be considerably affected by the soil-structure interaction (SSI) phenomenon which is strongly dependent upon the structure and the soil conditions and the associated parameters [3-5].

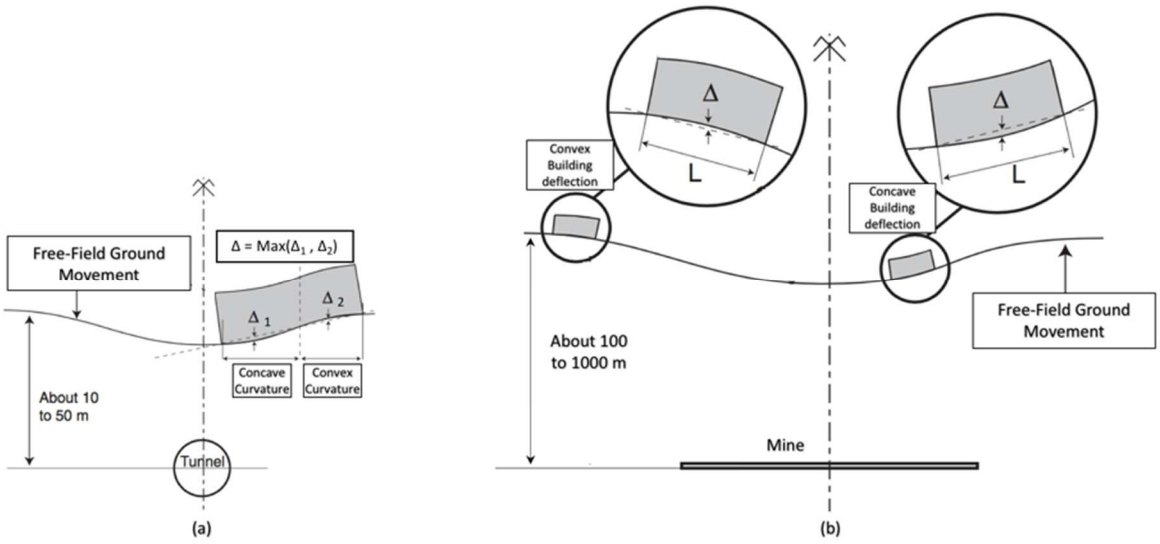

Figure 1. Building deflection caused by ground movements: (a) Case of tunneling. (b) Case of underground mine.

By neglecting the impact of the interaction between the soil and the structure, the free-field ground movements are integrally transmitted to the building. Under this assumption, Δ_0 represents the maximum deflection of the building. Assuming that the free-field ground movement is symmetrical and roughly circular under the building, Δ_0 represents the maximum free-field deflection under the building (for an integrally transmitted movement); it depends upon the ground radius of curvature R and the building length L (Figure 2).

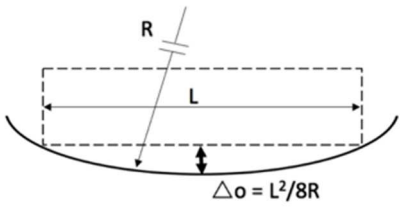

Figure 2. Free-field deflection Δ_0.

By considering the impact of the SSI, the soil, located under an existing structure and subjected to a ground movement, will influence the structure differently due to the interdependence of the mechanical behavior between the soil under the foundations and the structure sitting on these foundations. This interdependence is strongly dependent on the stiffness of the structure as well as that of the soil [2, 4, 6]. Due to the influence of the SSI, the ground movement may be partially transmitted to the structure which results in a building deflection characterized by its maximum value Δ with $\Delta \leq \Delta_0$. As shown in Figure 3, if the structure is stiff, it can resist the ground movement and the induced transmitted deflection is limited ($\Delta < \Delta_0$); if it is flexible, then it perfectly follows the settlement of the soil and $\Delta = \Delta_0$.

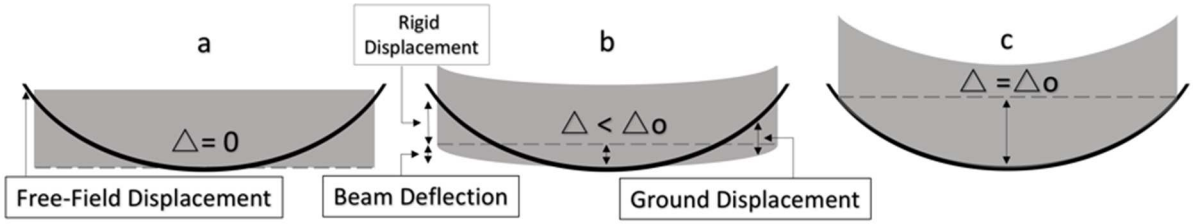

Figure 3. Behavior of structures subjected to ground movement. (a) High-stiffness structure on soft ground. (b) Intermediate ground and structure stiffness. (c) Flexible structure on stiff ground.

For a symmetrical free-field movement with respect to the structure, the deflection Δ corresponds to the maximum differential settlement under the building. For a non-symmetrical free-field movement case, Δ represents the maximum deflection of the building, whether the structure has a concave or a convex deformation (Figure 1-a).

The Δ / L ratio, called the deflection rate, is frequently used to assess the behavior of structures subject to differential settlement and to evaluate their damage [6, 7]. Since the damage depends upon

78 the rate of movement transmitted to the building, the structure response to the ground movement is
79 usually evaluated through the deflection transmission ratio, defined as Δ/Δ_0 [8, 9].
80 Different methods (analytical, numerical, experimental, empirical field data results) have been
81 developed to predict the building deflection in response to the ground movements [6-15]. Except
82 empirical methods that are based on observations of real existing structures, all of these methods do
83 not consider a specific study of a particular case but they are applied to simplified structures, such as
84 beams, in order to assess the global trend of ground movements induced phenomena.
85 Among the approaches developed to study the SSI phenomenon, only numerical methods offer great
86 flexibility for taking into account the complexity of the SSI conditions [11, 16]. Although it is
87 relatively simple to consider complex soil and structure behaviors in numerical models, their use may
88 be criticized by the justification of the numerical values of all parameters and conditions. In addition,
89 numerical models present difficulties to generalize results, because of the need to reproduce the same
90 scenario numerous times, by varying a particular SSI parameter in each repetition to cover the extent
91 of the variation range of all parameters. Thus, they can be considered as time-consuming processes
92 [7].
93 To avoid these difficulties, it is possible to obtain results through analytical methods that develop
94 simple equations that represent the structural deflection. Analytical methods may be considered as a
95 complementary tool to the numerical ones, allowing quick calculations for a wide variation range of
96 parameters, without considering complex configurations [6]. In these analytical models, the soil is
97 modelled with simple elastic stiffness elements as elastic springs. Winkler model is the simplest soil
98 model and has been used by many investigators and by Deck and Singh (2010) [7] to address the
99 question of the building deflection induced by ground movements and the assessment of Δ/Δ_0. Such a
100 SSI model can be criticized because it neglects any interaction between the springs and because it
101 assumes a purely elastic behavior of the ground [17]. As a consequence, it does not take into account
102 the influence of soil settlement outside the loaded area, which leads to discontinuities in the settlement
103 profile when the applied load is also discontinuous; the displacements of the soil outside the building
104 are supposed null, which is not correct. Basmaji et al. (2017) [6] developed a similar SSI model by
105 replacing the Winkler by Pasternak model in order to introduce some interactions between the springs

(Figure 4). This SSI model corrects some critical points of the previous one, but it does not take into consideration the soil elastoplastic behavior.

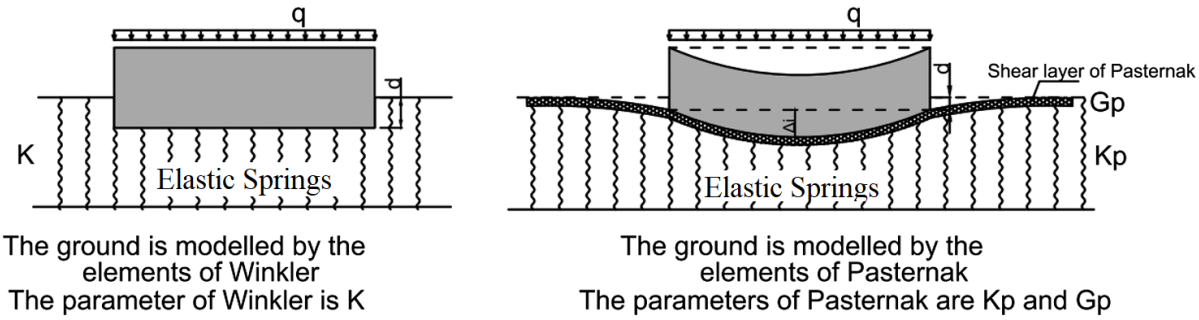

Figure 4. Structure on a soil modelled analytically with the one parameter Winkler's elastic model or the two parameters Pasternak's elastic model.

Thus, soil analytical models do not take into account the influence of the soil elastoplastic behavior even-though this factor significantly affects the transmission of ground movements to structures [6-9]. As shown in Figure 5, the target of this paper is to investigate the influence of soil elastoplasticity on the transmission of ground movements affecting the soil-structure interaction. Based on the elastic analytical models, a simplified elastoplastic meta-model is proposed, via statistical regressions, to evaluate the structural response. A modification is added to the analytical elastic models that assimilate the soil to a juxtaposition of elastic springs; the modification incorporates elastoplastic conditions based on the soil bearing capacity. Results of the analytical approach are then compared to the results obtained by numerical finite element models. In order to generalize the obtained results, a large database of the deflection transmission ratio is evaluated for different combinations of the SSI parameters and the soil bearing capacity. Based on this database, a new correlation is proposed to evaluate the transmission of ground movements to structures considering the elastoplastic soil behavior, in an effort to improve the investigation of the structure response to ground movements.

Step 1 $(\Delta/\Delta_0)_{Elastic}$		**Step 2** **Elastoplasticity**		**Step 3** **Validation**		**Step 4** **Reduction Coefficient**
Evaluate the transmission ratio $(\Delta/\Delta_0)_{Elastic}$ analytically based on soil elastic models.	→	Incorporate elastoplastic conditions based on the soil bearing capacity	→	Validate the analytical results by the numerical finite element models.	→	Generalize the results of the transmission ratio $(\Delta/\Delta_0)_{Elastoplastic}$ by considering the soil elastoplastic behavior through a reduction coefficient.

Figure 5. Diagram representing the study plan.

2. Procedure & Modeling

Previous research on this subject addresses the question of building stiffness compared to ground stiffness, which is known as "relative stiffness", and suggests to assess the transmission ratio Δ/Δ_0 as a function of a relative stiffness parameter ρ* between the soil and the structure [7, 11, 18].

Most of these studies rely on Eq. (1) to evaluate the relative stiffness parameter ρ* based on the structure length L, inertia I, Young's modulus E and the soil Young's modulus Es. Since it is a 2D study done per linear meter (EI [N.m^2/m]), Eq. (1) has the advantage of being non-dimensional and of being well adapted to a synthetic representation of Δ/Δ_0.

$$\rho* = \frac{EI}{EsL^3} \quad (1)$$

In order to propose a simplified meta-model that evaluates the transmission ratio Δ/Δ_0 as a function of the relative stiffness ρ*, an appropriate SSI model has to be considered. While there is a significant number of SSI models proposed in the literature [6-8, 10-11, 18-23], a comparison between two elastic models, representing the transmission ratio Δ/Δ_0 versus the relative stiffness ρ* for a wide variation range of SSI parameters, is performed.

2.1. Elastic Deck & Singh SSI analytical model

Deck and Singh (2010) [7] developed a SSI analytical model to calculate the deflection transmission ratio Δ/Δ_0 as a function of the ground and building mechanical properties. As shown in Figure 6, the building is assimilated to an elastic Euler–Bernoulli beam and the ground is represented by the Winkler model, which consists on assimilating the soil to a juxtaposition of vertical springs characterized by their stiffness K without any interaction between them. Considering that p(x) and w(x) represent the ground reaction and displacement respectively, Winkler model is evaluated using Eq. (2). The ground is modelled with an initial shape corresponding to Δ_0 and a polynomial equation v(x) (Eq. (3)) that represents the free-field movement shape. The final building deflection Δ is then calculated based on the final position and deformation of the beam required to get a static equilibrium under its own weight q and the vertical ground reaction p(x) (Eq. (4)).

$$p(x) = Kw(x) \quad (2)$$

$$v(x) = \Delta_0 (1\text{-}4x^2/L^2) \quad for \quad -L/2 < x < L/2 \tag{3}$$

$$y^{(4)}(x) = \frac{q - p(x)}{EI} \tag{4}$$

Where L and EI are the building length [m] and elastic stiffness [N.m2/m] (since it is a 2D study done per linear meter).

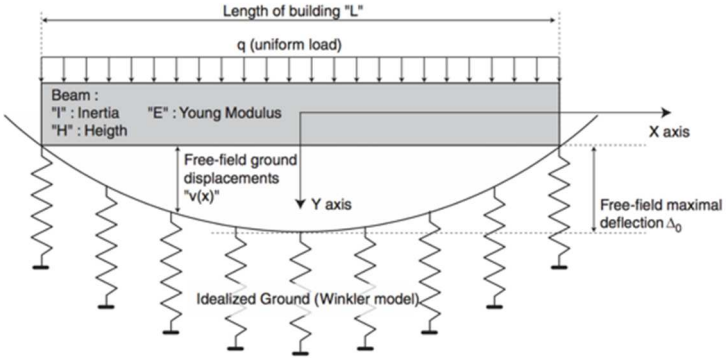

Figure 6. Deck & Singh (2010) analytical model for the SSI and the building deflection induced by ground movements.

On the other hand, Deck & Singh (2010) [7] introduced their own relative stiffness definition to plot the results of Δ/Δ_0 (Eq. (5)) that is suitable to the Winkler model, since the ground stiffness is defined with the Winkler parameter K instead of Es used in Eq. (1).

$$\rho * (Deck\ \&\ Singh) = \frac{EI}{KL^4} \tag{5}$$

Where K is the Winkler elastic modulus [N/m^3].

This equation is comparable to other relative stiffness ratios defined in the literature; it presents the advantage of being a non-dimensional parameter and suitable to have a synthetic representation of Δ/Δ_0 based on Winkler model. In order to show the consistency between Eq. (1) and Eq. (5), Vesic (1963) [24] formula (Eq. (6)) is used to define values for K in the case of a foundation with length L, width B (with L>B) and a ground characterized by a Young's modulus Es and a Poisson's ratio υ. In this case B is taken equal to 1m, which approximatively corresponds to the width of a building foundation. Noting that various formulas link the Winkler modulus to the soil Young modulus [24-28], Vesic formula is chosen since it takes into account the presence of a beam (through the "EI" term) contrary to other formulas.

$$K = \frac{0.65Es}{B(1-\nu^2)} \sqrt[12]{\frac{EsB^4}{EI}} \tag{6}$$

Figure 7 shows the Deck & Singh (2010) results for the transmission ratio plotted against the relative stiffness ρ*(Deck & Singh) defined in Eq. (5). A comparison is done between the Δ/Δ_0 values evaluated according to specific values of K and Δ/Δ_0 values evaluated according to specific values of Es and converted to K according to Vesic formula (Eq. (6)). The difference between the results is slight (Figure 7) which validates the consistency between Eq. (1) and Eq. (5) using Vesic formula.

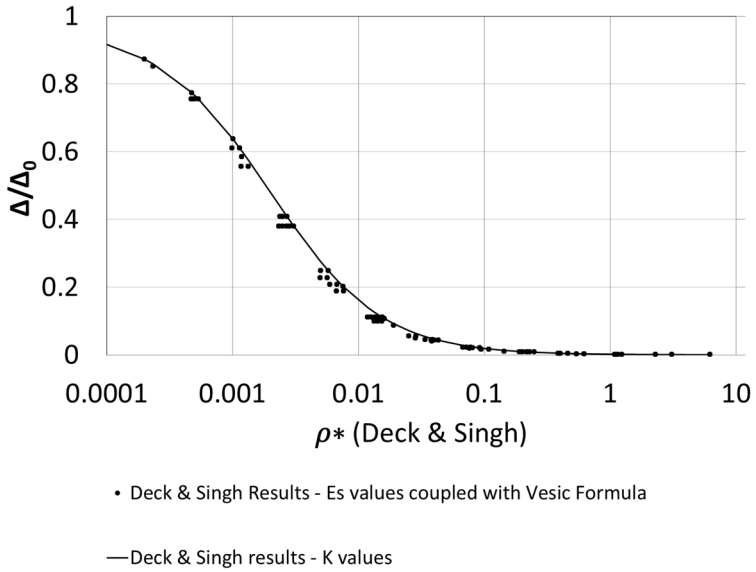

Figure 7. Results of the deflection transmission ratio Δ/Δ_0 versus the relative stiffness ratio ρ*(Deck & Singh) obtained for K values and for Es values coupled with Vesic formula.

2.2. Elastic Basmaji et al. SSI analytical model

Based on Deck & Singh (2010) model, Basmaji et al. (2017) [6] developed their analytical model where the soil is represented by the Pasternak model, a two parameters soil model that takes into account the interaction between adjacent springs, in addition to the influence of shear deformation in the soil (Figure 4). The two parameters are the shear modulus Gp, and the stiffness modulus Kp. The soil reaction can be written as follows:

$$p(x) = K_P.B.w(x) - G_P.B.w''(x) \qquad (7)$$

When Gp is taken to be zero, the Pasternak model is equivalent to the Winkler model. The Winkler parameter K is used instead of Kp. It should be noted that if a given geotechnical problem is modelled with each of the two models, i.e., Pasternak and Winkler, the values of Kp and K will be different, unless Gp is assumed to be equal to zero [6].

As shown in Figure 4, due to the influence of the shear layer, Pasternak model displays a differential settlement under the building without any discontinuities contrary to Winkler model that displays a uniform settlement with a discontinuity at the edge. Thus, when a local force F acts on a point (x) of a soil modelled by Pasternak model, the slope curve w'(x) presents a discontinuity. Conversely, any discontinuity of w'(x) must be associated to a local force. To overcome this problem, Eq. (7) must be completed with Eq. (8).

$$F = w'_{left}(x) - w'_{right}(x) \qquad (8)$$

Where w'_{left} and w'_{right} are the limit of the first derivatives of w(x) for x_0- and x_0+ respectively and F is the associated local force (Figure 8).

To highlight the effect of the shear deformation, Basmaji et al. (2017) compared Pasternak and Winkler models. In order to make a suitable comparison, the transmitted ratio Δ/Δ_0 has to be plotted versus the same definition of the relative stiffness ρ^*. To do so, the parameters used in the soil models have to be calculated according to the same methodology in order to correspond to the same soil in terms of Young's modulus and Poisson's ratio. Due to the lack of existing analytical relations to assess the two parameters used in the Pasternak's model (Gp and Kp), Basmaji et al. (2017) [6] implemented a new methodology based on Flamant's theoretical solution of induced vertical settlement. They adjusted the displacement for both methods according to Flamant's theoretical solution in order to justify the parameter values for Winkler and Pasternak. Consequently, they proposed abacuses to select the Winkler and Pasternak values based on the half width of the loaded zone and the thickness of the compressive ground for Es = 1MPa and ν = 0.3. However, the comparison of the transmitted ratio Δ/Δ_0 versus the relative stiffness ratio ρ^* defined in Eq. (1), between Pasternak and Winkler models, reveal a discrepancy between both methods which is related to the influence of shear deformation into the soil (Figure 10).

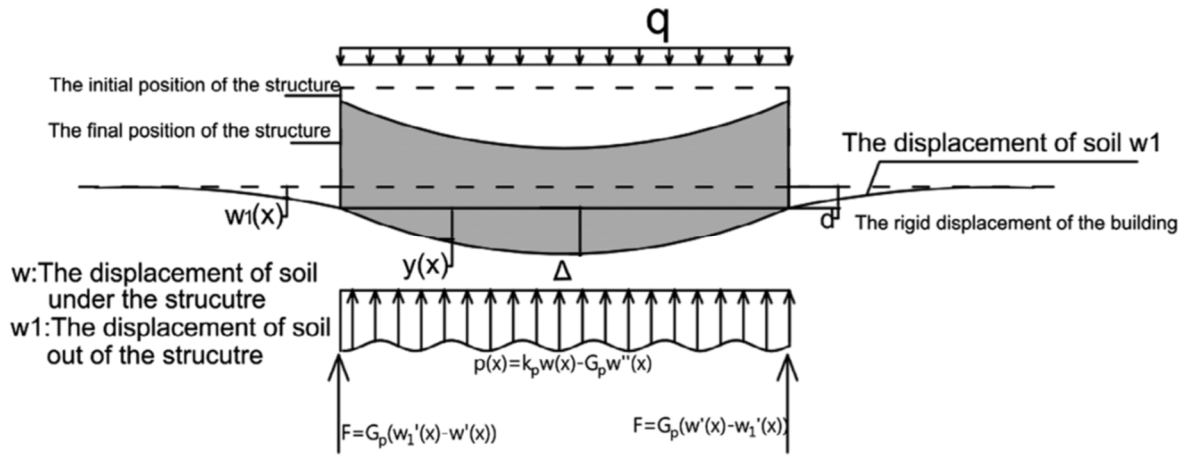

Figure 8. Definition of parameters used to model the beam deflection according to Pasternak model.

2.3. Validation of elastic analytical models

A significant number of SSI models (analytical, numerical, experimental, etc.) were proposed in the literature. In order to investigate the influence of soil elastoplasticity on the transmission of ground movements, the elastic analytical models have to be validated, since a simplified elastoplastic meta-model will be proposed based on the elastic analytical results. Two validation techniques are evaluated in this paper: (a) Validation with a finite-element model; (b) Validation with numerical, experimental and field data results from previous research.

2.3.1. Validation with a finite-element model

A finite element model (FEM) is developed to compare the elastic analytical results with a set of numerical simulations. The objective of the FEM is to model the ground curvature induced by ground movements and calculate the transmission ratio of the free-field deflection. In fact, Basmaji et al. (2017) [6] and Deck & Singh (2010) [7] validated their analytical results with numerical models; however, they considered an elastoplastic ground behavior in their studies, and they modeled the subsidence by a uniformly distributed load imposed on the lower boundary. On the contrary, the numerical model presented in this paper intends to fully reproduce the analytical conditions in order to well verify the effectiveness of the analytical results. Subsequently, this FEM model considers an elastic ground behavior and the subsidence is imposed without adding a uniform load on the lower boundary.

The numerical model is performed with a finite element software (Plaxis 2D) under the plane strain hypothesis. The model consists of an elastic soil layer, 125 m thick and 800 m long, with a building located at the center (Figure 9). For the boundary conditions, the horizontal displacement is fixed on the right and left boundaries and the vertical displacement is fixed only at the bottom boundary right and left sides (L1) while the central region of the bottom boundary is free. So, to model the subsidence and the free-field displacement, the length of L1 is selected in order to reach a value of Δ_0 that is equivalent to the analytical model.

The soil Poisson's ratio ν is 0.3 and the unit weight is 20 KN/m^3. The structure is modeled by a beam that is loaded with a vertical uniformly distributed load q. Mechanical properties and buildings dimensions are chosen in order to get values that are identical to the ones considered in the analytical approach (EI and L).

(a) A first computation is performed by fixing the vertical displacement on all the lower boundary in order to generate the initial ground situation under the soil weight; all the evaluated displacements are then set to zero.

(b) A second computation is performed by fixing the vertical displacement on L1, without considering the structure, in order to assess the free-field displacement Δ_0 of the subsidence; Δ_0 is evaluated and the displacements are set to zero.

(c) A third computation is performed with the precense of both the structure (with the vertical uniformly distributed load) and the subsidence in order to assess the final building deflection Δ considering the soil-structure interaction.

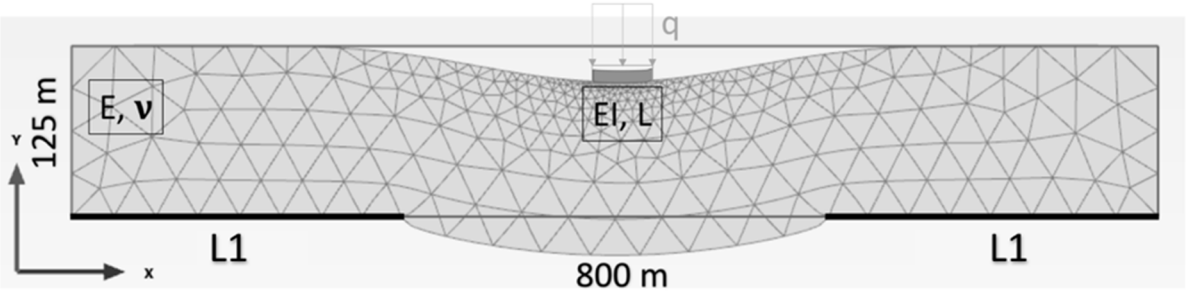

Figure 9. Description of the finite element model used to compare analytical results of the deflection transmission ratio with numerical results.

A set of 10 simulations are performed that cover the distribution range of the relative stiffness ρ^*, for

different values of EI/B, Es, L, q and Δ_0. Globally, numerical results presented in Figure 10 are superimposed with the curve of the transmission ratio calculated with the elastic analytical models of Deck & Singh (2010) Winkler model combined with Vesic (1963) formula and Basmaji et al. (2017) with Pasternak model; consequently, these two analytical approaches seem to be sufficient to predict the trend of the transmission ratio.

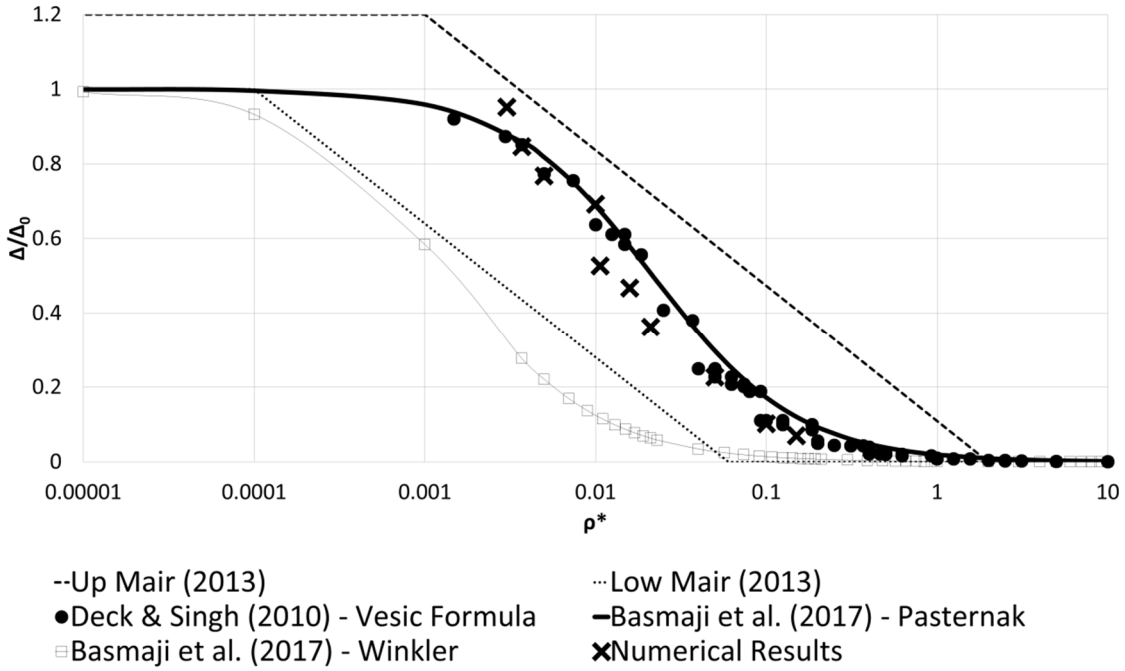

Figure 10. Comparison between Mair, 2013; Deck & Singh, 2010; Pasternak-Basmaji et al., 2017; Winkler-Basmaji et al., 2017 and numerical results.

2.3.2. Validation with numerical, experimental and field data from previous research

In addition to the finite-element model validation, Mair (2013) [2] envelope is used to validate the elastic analytical results. In fact, Mair (2013) [2] compared the transmission ratio, derived from the finite-element analyses of Potts and Addenbrook (1997) [11] and Franzius et al. (2006) [29] with respect to the relative stiffness. Also, he considered the results of the finite element parametric analyses, of deep excavations in soft clay on adjacent buildings, using the Modified Cam Clay soil model done by Goh (2010) [30]. The comparison of these studies shows that the obtained results fall into a relatively narrow envelope known as Mair (2013) [2] envelope (Figure 10).

As shown in Figure 10, the elastic analytical models of Deck & Singh (2010) with Winkler model [7] combined with Vesic (1963) formula and Basmaji et al. (2017) with Pasternak model [6] fit well

within Mair (2013) envelope, while an important discrepancy is shown between these results and Basmaji et al. (2017) with Winkler model [6]. Accordingly, even-though Deck & Singh (2010) Winkler model does not consider the shear deformation and the displacement outside the building, results show that the influence of these properties is indirectly taken into consideration or compensated by evaluating the Winkler modulus according to Vesic (1963) formula. In fact, Vesic (1963) has adopted the principle of equivalence between two solutions to find the soil reaction modulus for an infinite length beam in contact with the ground, modeled by the Winkler model. The same principle has been adopted by Basmaji et al. (2017) to calculate the Pasternak parameters; it was done for the case of a distributed load applied on a length L on a soil modeled by the Pasternak model. Thus, the results of Deck & Singh (2010) Winkler model combined with Vesic (1963) formula and Basmaji et al. (2017) with Pasternak model are comparable.

3. Results & Discussion

3.1. $(\Delta/\Delta_0)_{Elastic}$

Based on Eq. (4), the Deck & Singh analytical model is based on evaluating the deflection of the building using Euler–Bernoulli forth order differential equation. To solve the problem, six boundary conditions are used which present computation difficulties and time consumption to generalize the results for a significant number of iterations. On the other hand, as shown in Figure 8, Pasternak model presents punctual forces at the building extremities; thus, a higher number of boundary conditions is needed for Basmaji et al. (2017) model leading to additional computation time difficulties.

In order to simplify the evaluation of Δ/Δ_0, this paper proposes simple meta-model equations, based on the results shown in Figures 7 and 10, depending upon the relative stiffness ρ^* parameters, namely the structure stiffness EI and length L and the soil stiffness Es that can be substituted by the soil modulus K evaluated according to the Vesic formula (Eq. (6)). A significant number of iterations of the ρ^* parameters is evaluated, covering its variation range in the analytical models of Deck & Singh (2010) and Basmaji et al. (2017). Since these original models are heavy to implement and expensive in computation time, polynomial meta-models are proposed to evaluate $(\Delta/\Delta_0)_{Elastic}$. The predictability

and general applicability of the equation are evaluated by comparing the predictions of these meta-models with analytical results of the original models. Thus, the meta-models allow having, in any point of the design space, an estimate of the value of the elastic transmission ratio $(\Delta/\Delta_0)_{\text{Elastic}}$ while reducing the computation time for designers and engineers. Based on Figure 7 and Figure 10, Eq. (9) and Eq. (10) correspond to $(\Delta/\Delta_0)_{\text{Elastic}}$.

$$\frac{\Delta}{\Delta_0}\text{Elastic}(\text{EI}, \text{K}, \text{L}) = 0.5 - 0.5\,Tanh[2.99373 + 0.46898\,(\frac{EI}{KL^4})] \quad (9)$$

(K evaluated according to the Vesic formula)

$$\frac{\Delta}{\Delta_0}(\text{EI}, \text{Es}, \text{L}) = 0.5 - 0.5\,Tanh[1.96633 + 0.512843\,(\frac{EI}{EsL^3})] \quad (10)$$

3.2. Integrate the elastoplastic soil behavior

The objective is to develop an analytical SSI model that takes into account the influence of plasticity in the soil. To consider the influence of the elastoplastic soil behavior, a comparison between the stresses applied to the soil and its bearing capacity will be used as a criterion to judge whether the soil is in a plastic state or not. If it is in a plastic state, a new relation is proposed based on assuming that the vertical stresses in the soil must not exceed the bearing capacity of the soil (Figure 11). If the applied forces exceed the soil bearing capacity, a spring continues to deform but it cannot carry any additional stress. The overloads are thus transferred to nearby springs which are still in the elastic range. The applied procedure is iterative given the nonlinear behavior of the ground.

As presented in Figure 11, at the beam edges where the constraints are greater than p_{ult} , $p(x)=p_{ult}$ is imposed. Note that, since the integral of p(x) before and after taking into account the plasticity is always equal to the external loads applied to the building, the values of p(x) are increased in the middle of the beam for the elastoplastic behavior, as shown in Figure 11.

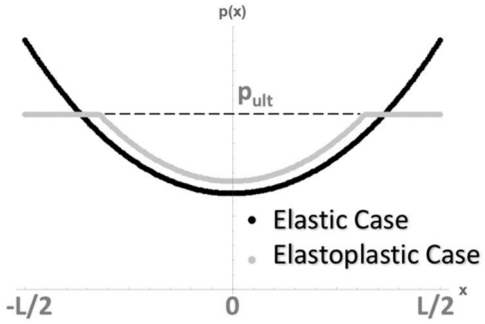

Figure 11. Presentation of the applied procedure.

The concept of considering the elastoplastic soil behavior is divided into two cases (elastic and elastoplastic) as follows:

Elastic Case:	Winkler	$p(x) = K.w(x)$	*(2)*
	Pasternak	$p(x) = K_P.B.w(x) - G_P.B.w''(x)$	*(7)*
Elastoplastic Case:		$p(x) = p_{ult}$	*(11)*

Where p_{ult} is the soil bearing capacity; p_{ult} is the maximum stress that the springs can carry. First, the elastic conditions of Winkler and/or Pasternak are considered (Eq. (2) or Eq. (7)). Then, the beam deformation and the stresses applied to the ground are evaluated. Two cases are then possible:

- The stresses applied to the ground are less than p_{ult} (the soil is still in the elastic range). In this case, the maximum deformation of the building can be directly evaluated according to Winkler and/or Pasternak equations.
- Some of the stresses applied in a certain zone under the building (at the edges), known as the "plastic zone", are greater than p_{ult}. In this case, an iterative procedure is applied to find the solution in the plastic zone and determine the soil reaction based on Eq. (11).

3.2.1. Winkler model

An example is presented to show the influence of considering soil plasticity. This example is based on the model considered by Basmaji et al. (2017) [6] with an additional parameter (the soil bearing capacity), in order to integrate the elastoplastic conditions. Given a beam of unit width and length L=20m, stiffness EI=5350MN.m^2, loaded with 100KN/m, bearing capacity p_{ult}=120KN/m, Winkler

reaction modulus K=3850KN/m^3 and a radius of curvature of the free field ground movement R=1500m, the solution of the problem is found by solving the equations and boundary conditions using Mathematica.

Figure 12 first shows the elastic solution for which there is no limitation on the soil reaction due to assuming an elastic behavior for the soil. For this case, the maximum displacement in the middle of the building is equal to 0.6 cm. However, at the boundaries there is an area where $p(x) > p_{ult}$, then the soil plasticity must be considered. Consequently, by applying the iterative process of resolution (Eq. (2) and Eq. (11)), it is noted that the maximum deflection of the beam Δ is reduced from 0.6 cm to 0.35 cm after considering plasticity.

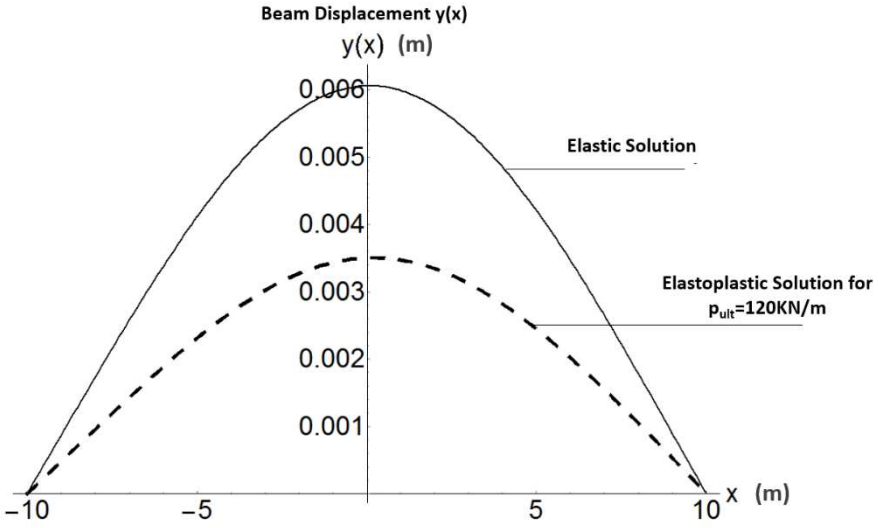

Figure 12. Vertical displacements at the soil-structure interface according to the elastic and elastoplastic behavior of the ground.

3.2.2. Pasternak model

A procedure similar to that applied to Winkler model, to find the solution of a beam on an elastoplastic ground, is applied to find a solution for Pasternak model. However, since there is a soil displacement in Pasternak model outside the structure length L, the solution must take into account the movements of the soil throughout the whole system. The system is composed of the ground under the structure of length L, and the ground outside the structure over a length of 5L. It is assumed that the displacement of the ground at a distance of 5L from the structure is zero, this distance being

infinite in the case of an analytical solution. The length 5L was chosen after numerous tests, as a reasonable compromise to obtain a satisfactory solution without an excessive computation time.

A preliminary example according to the Pasternak model has been applied and results show an inconsistency and a discontinuity in the values of the punctual forces at the building edges. According to the simulations evaluated by Mathematica, the soil reaction is concentrated in the two punctual forces generated at the building extremities. The value of F is significantly higher than the total sum of the reaction p(x) distributed under the building (Figure 8) which confirms the necessity of adding a limitation of the maximum punctual forces admissible at the building extremities. To do so, the shear modulus Gp is modified locally as per Eq. (12) so that the formula of the punctual force F shown in Figure 8 is limited by multiplying it by a coefficient α.

$$F_{lim} = \alpha \, \mathrm{Gp} \, (w'(x) - w'_1(x)) \tag{12}$$

The criterion of validation of the results is the verification of the stability of the system (statistical equilibrium of the system) for each iteration, as per the following equation:

$$qL = \int_{-L/2}^{L/2} p(x) + 2F \tag{13}$$

As shown in Figure 13, it is found that, without plasticity, the soil reaction p(x) decreases with the increasing values of x toward the beam edges where the punctual force F is located. However, after considering the influence of plasticity, the p(x) decreases at the beam center and increases at the beam edges in comparison with the first case. These results confirm the statistical balance and the equivalence between the sum of the reactions of p(x) and F from one side and the loads applied to the beam from the other side.

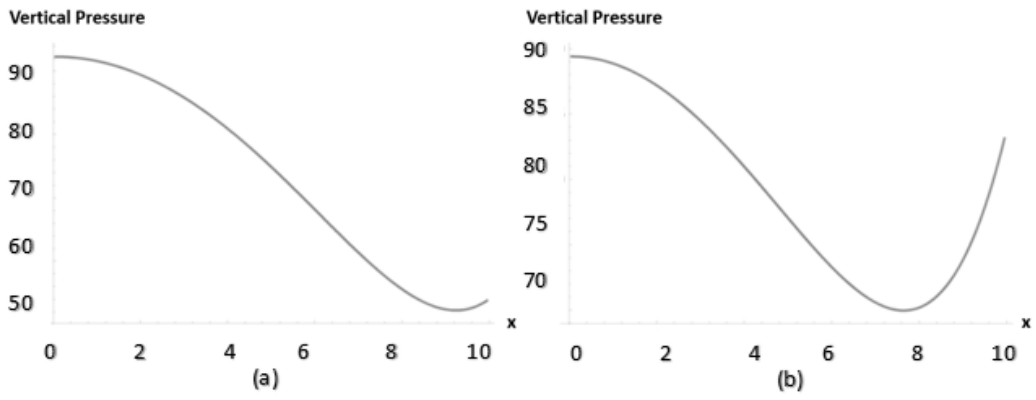

Figure 13. Vertical pressure along the half beam (a) without plasticity; (b) with plasticity.

In order to find the exact value of F_{lim} , the parameter α is varied from 0.1 to 0.7 with a step of 0.1 to find the suitable value of F where the sum of the soil reaction p(x) and F is exactly equal to the loads applied to the beam. The results obtained showed that a value of α= 0.4 seems to be the most adequate for the Basmaji et al. (2017) example shown in Figure 12.

However, even-though the elastoplastic soil conditions can be integrated to the Pasternak model, the applied procedure presents several difficulties since the coefficient α has to be evaluated for every case separately and to check the system stability and the equivalence between the sum of the reactions and the applied loads by varying the value of α progressively. Thus, the process of integrating elastoplastic conditions to the Pasternak model is time consuming and presents difficulties to be generalized. Since the objective is to propose a 'generalized' meta-model that integrates the soil elastoplasticity, this paper will proceed by considering the Deck & Singh (2010) Winkler model combined with Vesic (1963) formula.

3.3. Validation with finite-element models

Based on the elastic finite element model explained previously, a new elastoplastic model is developed on Plaxis 2D. This model consists of dividing the soil into two layers; the upper layer of thickness h1 = 100 m is modelled as elastoplastic with a Mohr–Coulomb criterion, whereas the lower layer of thickness h2 = 25 m is assumed to be elastic. The function of the upper layer is to represent the elastoplastic conditions with a cohesion and a friction angle that vary with respect to p_{ult} value determined by the Terzaghi formula:

$$p_{ult} = cN_c + 0.5B\gamma_1 N_\gamma + (q + \gamma_2 D)N_q \qquad (14)$$

with γ_1 the soil density under the foundation, γ_2 the soil density lateral to the foundation, q the lateral vertical overload to the foundation, c the cohesion of the soil under the base of the foundation, B the width of the foundation, D the embedment depth of the foundation and N_c, N_q, $N\gamma$ the bearing capacity factors.

The function of the lower layer (h2 = 25 m) is to avoid large deformations and large mass losses that occur near the lower limit due to the fact that such a loss could compromise the convergence of

calculations and the accuracy of results; also stress-strain results are only interpreted for the upper ground layer. Considering an elastoplastic soil layer in contact with the building, a sliding interface is modelled between the ground and the structure in order to investigate only the influence of the ground curvature and not the influence of horizontal strains and the associated shear stresses induced by the subsidence. The same boundary conditions are applied and the model is realized in three stages as for the elastic case.

The set of 10 finite-element models that were generated for the elastic conditions are evaluated for elastoplastic conditions considering a particular value of the bearing capacity p_{ult} (cohesion and friction angle as per Eq. (14)) for every case. The numerical results presented in Figure 14 are superimposed with the elastoplastic analytical results of the same considered combinations of the SSI parameters (same p_{ult}, EI, K, L, q and Δ_0 values) for the transmission ratio calculated with the Deck & Singh (2010) Winkler model combined with Vesic (1963) formula. Consequently, the analytical methodology developed to consider the soil elastoplastic behavior is validated numerically and can be used to predict the value of the elastoplastic transmission ratio $(\Delta/\Delta_0)_{Elastoplastic}$.

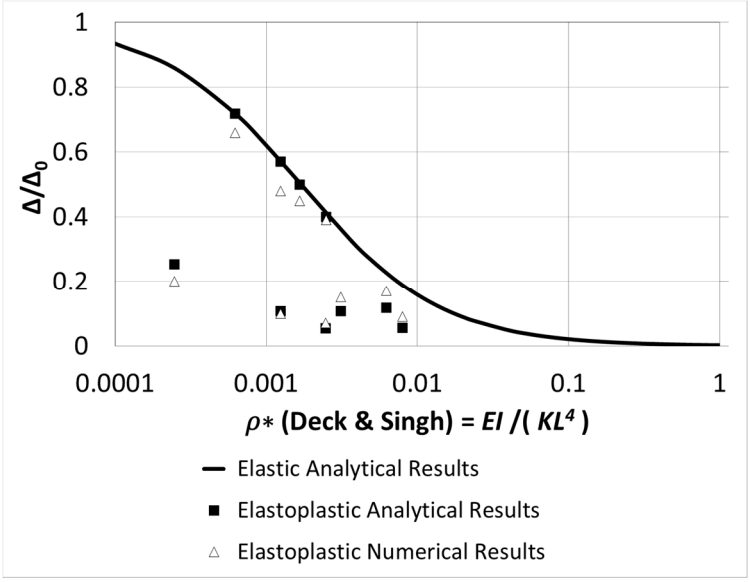

Figure 14. Results of the comparison between analytical and numerical results of the deflection transmission ratio.

3.4. Reduction coefficient

In order to study the effect of soil plasticity on the transmission ratio Δ/Δ_0, the elastoplastic analytical model was evaluated using Mathematica, by investigating 18,900 possible combinations of p_{ult}, EI, K,

L, R and q, as shown in Table 1.

The building length is taken between 10 and 30 m to model small and intermediate buildings [8]. The beam loading represents the building self-weight and service loading. 100 kN/m is approximately the weight of a 5 m high wall with a thickness of 0.5 m with service loading, 200 kN/m is approximately the weight of a 10 m high wall with a thickness of 0.5 m and 400 kN/m is about the weight of a whole building with three 5 m tall walls with a thickness of 0.5 m including service loading.

The beam bending stiffness EI is between 20 and 500 GN.m^2. The smallest value represents the stiffness of a 0.5 m masonry wall thickness with 5 m height and a 3000 MPa equivalent Young's modulus for the masonry. The largest value represents the stiffness of a 0.2 m thick concrete wall, 12 m tall with a 20000 MPa equivalent Young's modulus.

The ground stiffness values vary between 20 and 500 MPa, according to Eq. (6), for values of soil Young modulus between 40 MPa (soft ground) and 500 MPa (stiff ground) and a Poisson's ratio of 0.3. The free-field ground radius of curvature is set between 250 and 5000m to represent a wide range of scenarios [7].

Considering that the structures are usually constructed with shallow foundations of length L and width B with L >> B, the bearing capacity can be obtained by Terzaghi's formula which depends essentially on the angle of internal friction and the cohesion of the ground under the foundation. To show the essential role that the limitation of the soil bearing capacity can have on the deflection of the building, the soil bearing capacity is considered variable between q and 4 q. Nevertheless, given the partial safety factors used in construction codes (Eurocode, etc.) for the design of the foundations at the Ultimate and Serviceability Limit States ULS and SLS (1.35 or 1.5), the considered cases (pult = Xq with X = 1, 1.5, … , 4) can be representative to approximate to standard situations [4].

Table 1: Model Parameters.

Symbol (Unit)	**Description**	**Values**
L(m)	Beam Length	10, 20, 30
q(KN/m)	Beam Load	100, 200, 300, 400
p_{ult}	Soil Bearing Capacity	q, 1.5q, 2q, 2.5q, 3q, 3.5q, 4q
EI(GN.m^2)	Beam Stiffness	20, 50, 100, 250, 500
K(MPa/m)	Ground Stiffness	20, 50, 100, 250, 500
R(m)	Free-Field Ground Radius of Curvature	250, 500, 750, 1000, 1500, 2000, 3000, 4000, 5000

Based on the results shown in Figure 15 for the 18,900 investigated combinations, a new relation can be proposed for the elastoplastic deflection transmission ratio using a reduction coefficient "a" as follows:

$$\frac{\Delta}{\Delta_0}(\text{Elastoplastic}) = a\ \frac{\Delta}{\Delta_0}(\text{Elastic}) \qquad (15)$$

$$\text{With } 0 \leq a \leq 1$$

If a=1, p_{ult} is not reached with the soil still in the elastic range, and there is no difference between considering an elastic or an elastoplastic soil behavior. However, when "a" decreases below 1, p_{ult} is reached. In order to establish a new correlation that evaluates "a" as a function of p_{ult}, q, R, K, EI and L, the influence of every factor on "a" is evaluated and presented in Table 2.

Table 2: Effect of every increasing factor on a.

Factor	Comments	a
$\mathbf{p_{ult}}$ ↑	The soil does not reach the plastic phase and behaves as an elastic soil.	↑
q ↑	Due to static equilibrium, the soil reaction p(x) increases and may reach p_{ult} at a certain position under the structure.	↓
R ↑	The soil reaction difference at the ends of the structure is limited. The soil reaction p(x) then remains low and does not exceed p_{ult}, in most cases.	↑
K ↑	The soil reaction increases as per Winkler formula and becomes closer to p_{ult}.	↓
EI ↑	The building has more stiffness and can sink in the soil which will increase the soil reaction until reaching p_{ult}.	↓
L ↑	The structure is more flexible and the soil reaction under the structure is more homogeneous and exceeds less often p_{ult}.	↑

After evaluating 18,900 combinations (Table 1) and calculating Δ/Δ_0 for an elastic and an elastoplastic soil behavior, a new correlation (Eq. (16)) is proposed for the reduction factor "a" using artificial neural networks via JMP software which is a software used for statistical analysis.

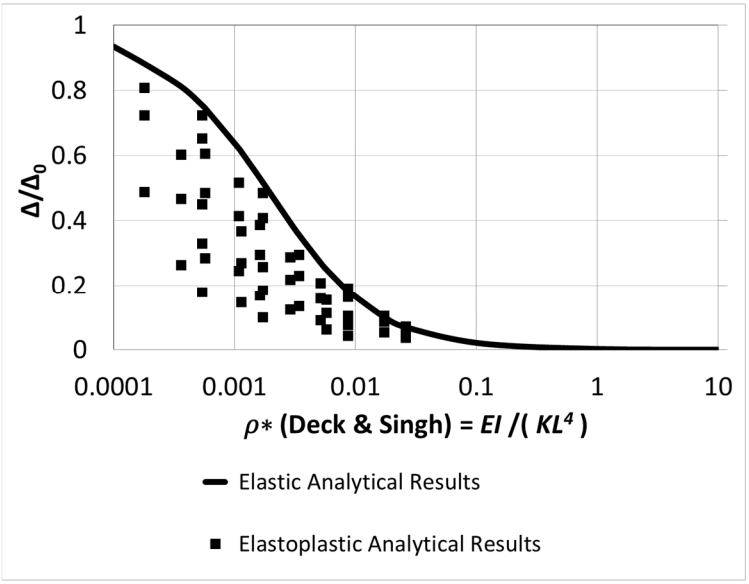

Figure 15: Deflection transmission ratio Δ/Δ_0 versus the relative stiffness ρ* for elastic/elastoplastic behavior of soil for various soil bearing capacities.

To obtain the analytic expression of a, several data analyzes were performed. Attempts to express this parameter by various combinations of the model input parameters have not lead to satisfactory results. For this reason, the technique of neural networks has been used [4, 31].

The artificial neural network is composed of a collection of artificial neurons by computing a weighted sum of the inputs (18,900 combinations of p_{ult}, q, R, K, EI and L). Many variations exist in the way neurons are organized into a network, but all neural networks are composed of multiple layers; an input layer, an output layer, and intermediate layers, called hidden layers. The proposed model seeks to match the relationship between the obtained values of Δ/Δ_0 and the inputs. For good generalization performance, a balance must be found between an artificial neural network with insufficient neurons that miss trends, and an artificial neural network with too many neurons that suffer from over fitting to the training data. The latter occurs when the minimization procedure tunes the weights in such a way that it almost perfectly captures the provided data, but is inaccurate when applied to new data, not used in the training procedure. To detect over fitting, the data is divided into three sets: a training, validation and test set. The network is built with a validation rate of 0.1 meaning that a proportion of 10% is therefore retained for validation. The final network obtained is composed of one layer and 3 neurons H1, H2 and H3 evaluated by minimizing the variance of the residues (Eq. (16)).

$$a = -7.19258 - 0.97155H1 - 0.52479H2 - 8.10706H3 \quad (16)$$

$$H1 = TanH\left(0.5\begin{pmatrix}-5.55733\\+0.00045K_w\\-0.00062R\\+0.00037q\\+0.00040p_{ult}\\+0.20247L\\+0.010897EI\end{pmatrix}\right); H2 = TanH\left(0.5\begin{pmatrix}44.10233\\+0.02106K_w\\-0.00035R\\+0.00033q\\-0.00102p_{ult}\\-1.77733L\\-0.076137EI\end{pmatrix}\right); H3 = TanH\left(0.5\begin{pmatrix}-2.44438\\+0.000078K_w\\+0.000071R\\+0.001837q\\-0.001939p_{ult}\\-0.009696L\\-0.001588EI\end{pmatrix}\right) \quad (17)$$

Figure 16 shows the actual values as a function of the expected values of the coefficient a. Thus, it is possible to visualize the residues. The coefficient of correlation is R^2 = 0.9026 and the root mean square error (RMSE) is relatively low (0.12). Figure 16 shows that the formulation of "a" has a general tendency to overestimate the large values of "a" and to underestimate the small values of "a".

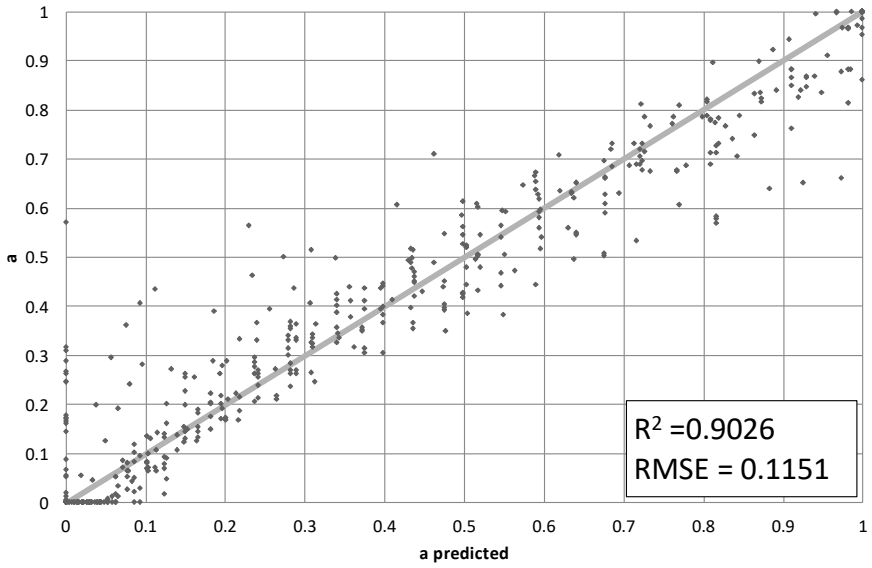

Figure 16: Graph of observed values versus expected values.

It should be noted that the network has been reconstructed with other values of the validation rate (0.2 and 0.3) and the results are roughly the same, the RMSE is always close to 0 and it slightly increases with the increase of this rate. Thus, results show that the application of Eq. (16) can approximate the influence of plasticity when evaluating the transmission ratio. Consequently, this correlation can be directly adopted by the engineering society for design purposes to approximate the Δ/Δ_0 value when considering the elastoplastic behavior of the soil.

4. Conclusions

This paper presents a new correlation to incorporate the elastoplastic soil behavior when evaluating

514 the transmission of ground movements to structures induced by tunneling and mining subsidence.
515 Based on the SSI analytical elastic approaches that are based on Pasternak and Winkler models, a new
516 methodology is implemented that consists of limiting the soil reaction to its bearing capacity in order
517 to consider soil elastoplastic conditions.
518 As shown in Figure 17, simplified equations are initially proposed to evaluate the elastic transmission
519 ratio $(\Delta/\Delta_0)_{Elastic}$ for (a) Deck & Singh (2010) Winkler model coupled with Vesic formula and (b)
520 Basmaji et al. (2017) Pasternak approaches. These two approaches are validated by elastic numerical
521 finite element models and numerical, experimental and field data results from previous research.
522 Then, the influence of soil plasticity on the transmission ratio Δ/Δ_0 is investigated by integrating the
523 soil bearing capacity p_{ult}. Results show a significant difference in the transmission ratio between the
524 elastic and the elastoplastic soil behavior. The elastic behavior results create an envelope that engulfs
525 the elastoplastic results.

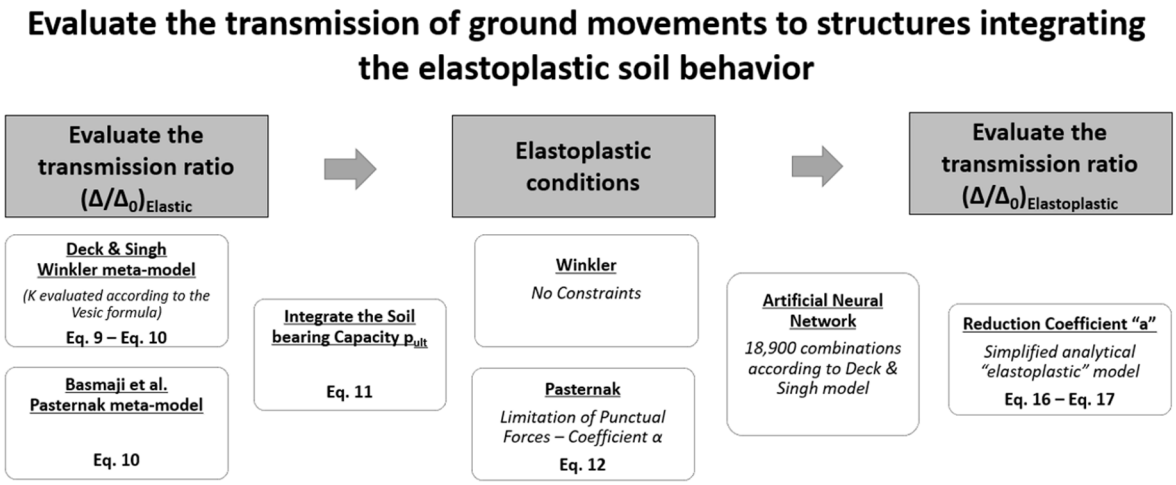

526

527 Figure 17: Methodology of evaluation of the new simplified meta-model to calculate the transmission
528 of ground movements to structures integrating the elastoplastic soil behavior.

529 On one hand, the proposed procedure applied for Pasternak model shows an inconsistency and a
530 discontinuity in the values of the punctual forces at the building edges. Thus, a coefficient α is
531 imposed to modify the shear modulus Gp locally and limit the maximum admissible punctual forces.
532 To find the value of α, it is required to check the statistical balance and the equivalence between the
533 sum of the reactions and loads applied to the beam for every combination. Thus, the proposed
534 procedure applied for Pasternak model is time consuming and presents difficulties to be generalized.

On the other hand, the proposed procedure applied for Winkler model (Deck & Singh model coupled with Vesic formula) does not show constraints and is validated by finite element-models.

Based on Deck & Singh Winkler model, a new meta-model is proposed that associates the elastic with the elastoplastic results of the transmission of the ground movement ($(\Delta/\Delta_0)_{Elastoplastic}$); the statistical meta-model is realized using artificial neural networks based on 18,900 combinations of SSI parameters and soil bearing capacities p_{ult}. A reduction coefficient "a" is proposed to associate the elastic ($(\Delta/\Delta_0)_{Elastic}$) with the elastoplastic ($(\Delta/\Delta_0)_{Elastoplastic}$) transmission ratios.

In conclusion, to improve the investigation of the structure response to ground movements and the evaluation of its damage, the effect of a significant SSI factor, the soil elastoplastic behavior, can be directly evaluated via the proposed simplified meta-model that is based on the elastic values of $(\Delta/\Delta_0)_{Elastic}$. To reduce time and calculation difficulties, this paper proposes simple equations (as shown in Figure 17) that are sufficient and can be directly used by geotechnical engineers and designers to consider the elastoplastic soil behavior and evaluate transmission of ground movements to structures.

Acknowledgment

The work presented in this paper was supported by a research grant from Lorraine University of Excellence and the National Council for Scientific Research-Lebanon (CNRS-L) and the Lebanese University.

References

[1] Mitropoulou, C., Kostopanagiotis, C., Kopanos, M., Ioakim, D. & Lagaros, N. Influence of soil–structure interaction on fragility assessment of building. *Structures*. 2016, 6: 85-98.

[2] Mair, R. Tunneling and deep excavations: Ground movements and their effects. *Proceedings of 15th European conference on soil mechanics and geotechnical engineering geotechnics of hard soils – weak rocks*; 2013, 4: 39-70.

[3] Anand, V. & Kumar, S. Seismic Soil-structure Interaction: A State-of-the-Art Review. *Structures*. 2018, 16: 317-326.

[4] ElKahi, E., Deck, O., Khouri, M., Mehdizadeh, R. & Rahme, P. Étude de l'influence de la plasticité du sol sur la transmission des mouvements du sol affectant l'interaction sol-structure. *Revue Française de Géotechnique*. 2018, 156, 4.

[5] Krishnamoorthy, A. & Anita, S. Soil–structure interaction analysis of a FPS-isolated structure using finite element model. *Structures*. 2016, 5: 44-57.

[6] Basmaji, B., Deck, O. & Alheib, M. Analytical model to predict building deflections induced by ground movements. *European Journal of Environmental and Civil Engineering*; 2017, 10: 1-23.

[7] Deck, O. & Singh, A. Analytical model for the prediction of building deflections induced by ground movements. *International Journal for Numerical and Analytical Methods in Geomechanics*; 2010, 36: 62-84.

[8] ElKahi, E., Khouri, M., Deck, O., Rahme, P. & Mehdizadeh, R. Studying the Influence of Uncertainties on the Transmission of Ground Movements Affecting the Soil-Structure Interaction. *10èmes journées Fiabilité des Matériaux et des Structures, Bordeaux, France*; 2018.

[9] Franza, A., Ritter, S. & Dejong, M. Continuum solutions for tunnel-building interaction and a modified framework for deformation prediction. *Géotechnique;* 2019: 1-15.

[10] Haji, K., Marshall, A. & Franza, A. Mixed empirical-numerical method for investigating tunneling effects on structures. *Tunnelling and Underground Space Technology*; 2018, 73: 92-104.
[11] Potts, D. & Addenbrooke, T. A structure's influence on tunneling-induced ground movements. *Proceedings of the Institution of Civil Engineers – Geotechnical Engineering*; 1997, 125: 109–125.
[12] Aissaoui, K. Amélioration de la prévision des affaissements dans les mines à l'aide des approches empiriques, numériques et analytiques-Doctorate thesis, Institut National Polytechnique de Lorraine, Nancy, France; 1999.
[13] Hassoun, M., Villard, P., Alheib, M. & Emeriault, F. Soil Reinforcement with Geosynthetic for Localized Subsidence Problems: Experimental and Analytical Analysis. *International Journal of Geomechanics*. 2018, 18 (10).
[14] Goh, K. & Mair, R. Building Damage Assessment for Deep Excavations in Singapore and the Influence of Building Stiffness. *Geotechnical Engineering*. 2011, 42: 1–12.
[15] Farrell, R. & Mair, R. Centrifuge modelling of the response of buildings to tunnelling. *Proceedings of the Seventh International Symposium on Geotechnical Aspects of Underground Construction in Soft Clay, Rome*. 2011, 2: 549-554.
[16] Koneshwaran, S., Thambiratnam, D. & Gallage, C. Blast Response of Segmented Bored Tunnel using Coupled SPH–FE Method. *Structures*. 2015, 58-71.
[17] Rahgozar, N., Rahgozar, N. & Moghadam, A. Controlled-rocking Braced Frame Bearing on a Shallow Foundation. *Structures*. 2018, 16: 63-72.
[18] Son, M. & Cording, E. Evaluation of building stiffness for building response analysis to excavation-induced ground movements. *Journal of Geotechnical and Geoenvironmental Engineering*; 2007, 133: 995-1002.
[19] Giardina, G., Hendriks, M. & Rots, J. Damage Functions for the Vulnerability Assessment of Masonry Buildings Subjected to Tunneling. *Journal of Structural Engineering*. 2014, 141 (9).
[20] Franza A. & DeJong M. A simple method to evaluate the response of structures with continuous or separated footings to tunnelling–induced movements. *Congress on Numerical Methods in Engineering, Valencia, Spain*; 2017: 919-931.
[21] Giardina, G., Marini, A. Hendriks, M., Rots, J. Rizzardini, F. & Giuriani, E. Experimental analysis of a masonry façade subject to tunnelling-induced settlement. *Engineering Structures*. 2012, 45: 421-434.
[22] Saeidi, A. La vulnérabilité des ouvrages soumis aux aléas mouvements de terrains : développement d'un simulateur de dommages-Doctorate thesis, Institut National Polytechnique de Lorraine, Nancy, France; 2010.
[23] Giardina, G., DeJong, M. & Mair, R. Important aspects when modelling the interaction between surface structures and tunnelling in sand. *Geotechnical Aspects of Underground Construction in Soft Ground - Proceedings of the 8th Int. Symposium on Geotechnical Aspects of Underground Construction in Soft Ground*. 2014: 263-268.
[24] Vesic. Beams on Elastic Subgrade and Winkler's Hypothesis. *Proceedings of the 5th International Conference on Soil Mechanics and Foundation Engineering*; 1963, 845-850.
[25] Biot. Bending of an infinite beam on an elastic foundation. *Journal of Applied Mechanics*; 1937.
[26] Drapkin. Grillage beams on elastic foundations. *Proc. ASCE*; 1955.
[27] Klöppel & Glock. Theoretische und Experimentelle Untersuchungen zu den Traglastproblemen Biegeweicher, in die Erde Eingebetteter. Institutes für Statik und Stahlbau der Technischen Hochschule Darmstadt; 1970.
[28] Henry. The Design and Construction of Engineering Foundations. Chapman & Hall; 1986.
[29] Franzius, J., Potts, D. & Burland, J. The response of surface structures to tunnel construction. *Proceedings of the Institution of Civil Engineers, Geotechnical Engineering*; 2006, 159: 3–17.
[30] Goh K. Response of Ground and Buildings to Deep Excavations and Tunnelling-Doctorate Thesis, University of Cambridge, 2010.
[31] Shahin, M., Jaksa, M. & Maier, H. Artificial Neural Network Applications in Geotechnical Engineering. *Australian Geomechanics*. 2001, 36: 49–62.

Graphical Abstract